

Quantitative Comparison of Cortical Bone Thickness Using Correspondence-Based Shape Modeling in Patients With Cam Femoroacetabular Impingement

Penny R. Atkins,^{1,2} Shireen Y. Elhabian,^{3,4} Praful Agrawal,^{3,4} Michael D. Harris,^{5,6} Ross T. Whitaker,^{1,3,4} Jeffrey A. Weiss,^{1,2,3,4} Christopher L. Peters,^{1,2} Andrew E. Anderson^{1,2,3,7}

¹Department of Bioengineering, University of Utah, Salt Lake City, Utah 84112, ²Department of Orthopaedics, University of Utah, 590 Wakara Way Rm A100, Salt Lake City, Utah 84108, ³Scientific Computing and Imaging Institute, Salt Lake City, Utah 84112, ⁴School of Computing, University of Utah, Salt Lake City, Utah 84112, ⁵Program of Physical Therapy, Washington University School of Medicine, Saint Louis, Missouri 63110, ⁶Department of Orthopaedic Surgery, Washington University School of Medicine, Saint Louis, Missouri 63110, ⁷Department of Physical Therapy, University of Utah, Salt Lake City, Utah 84108

Received 12 April 2016; accepted 23 October 2016

Published online in Wiley Online Library (wileyonlinelibrary.com). DOI 10.1002/jor.23468

ABSTRACT: The proximal femur is abnormally shaped in patients with cam-type femoroacetabular impingement (FAI). Impingement may elicit bone remodeling at the proximal femur, causing increases in cortical bone thickness. We used correspondence-based shape modeling to quantify and compare cortical thickness between cam patients and controls for the location of the cam lesion and the proximal femur. Computed tomography images were segmented for 45 controls and 28 cam-type FAI patients. The segmentations were input to a correspondence-based shape model to identify the region of the cam lesion. Median cortical thickness data over the region of the cam lesion and the proximal femur were compared between mixed-gender and gender-specific groups. Median [interquartile range] thickness was significantly greater in FAI patients than controls in the cam lesion (1.47 [0.64] vs. 1.13 [0.22] mm, respectively; $p < 0.001$) and proximal femur (1.28 [0.30] vs. 0.97 [0.22] mm, respectively; $p < 0.001$). Maximum thickness in the region of the cam lesion was more anterior and less lateral ($p < 0.001$) in FAI patients. Male FAI patients had increased thickness compared to male controls in the cam lesion (1.47 [0.72] vs. 1.10 [0.19] mm, respectively; $p < 0.001$) and proximal femur (1.25 [0.29] vs. 0.94 [0.17] mm, respectively; $p < 0.001$). Thickness was not significantly different between male and female controls. Clinical significance: Studies of non-pathologic cadavers have provided guidelines regarding safe surgical resection depth for FAI patients. However, our results suggest impingement induces cortical thickening in cam patients, which may strengthen the proximal femur. Thus, these previously established guidelines may be too conservative. © 2016 Orthopaedic Research Society. Published by Wiley Periodicals, Inc. *J Orthop Res*

Keywords: disease process; FAI and morphology; bone; statistics

One in four people will develop hip osteoarthritis (OA) in their lifetime.¹ Within the last decade, femoroacetabular impingement (FAI) has been implicated as a primary cause of hip OA in young adults.^{2–5} Two distinct presentations of FAI have been identified: pincer, defined as overcoverage of the femoral head, and cam, characterized by an aspherical femoral head and reduced head–neck offset. While many patients present with both cam and pincer FAI deformities, the morphological features of cam FAI tend to result in accelerated joint degeneration.³ In particular, cam-type femoral morphology may shear the cartilage at the chondrolabral junction during flexion and internal rotation of the hip.^{6–8}

Cam FAI is treated by resection of bone in the region of the femur believed to be abnormally shaped; the specific location of this region varies among patients but is generally located in the anterolateral or superolateral region of the femoral head–neck junction.⁴ If the amount of resection is too conservative,

the underlying impingement may not be fully addressed, which is a common reason for revision surgery.⁹ However, too aggressive of a resection may lead to an iatrogenic femoral neck fracture.¹⁰ In previous studies, non-pathologic cadaveric femurs,¹¹ or generalized femoral anatomy,^{12,13} were used to evaluate the effects of resection depth and shape on femoral neck strength. However, use of non-pathologic cadavers and simplified anatomy may not accurately represent the biomechanics of the femur in cam FAI patients.

The density and shape of bone is modified by the mechanical environment.¹⁴ In the case of cam-type FAI, repetitive impingement may induce hypertrophy of the bone, which may manifest as increased cortical thickness. The cortex contributes to the majority of load bearing within the hip.¹⁵ Thus, it is important to establish a baseline understanding of cortical bone thickness in patients with cam-type FAI, especially over regions that may be resected during surgery. Theoretically, a thicker cortex in cam FAI patients could imply that resection limits based on analyses of non-pathologic cadavers and generalized anatomy are overly conservative.

True anatomical variation of biological tissues can be difficult to identify due to complex morphology. Radiographic or other image-based measurements serve as the foundation for diagnosing cam FAI.^{16–18} However, there is a high prevalence of radiographic

Conflicts of interest: None of the authors report conflicts of interest associated with the design, execution, and publication of this study.

Grant sponsor: National Institutes of Health; Grant numbers: R01-EB016701, P41-GM103545-17, R01-GM083925, R21-AR063844.

Correspondence to: Andrew E. Anderson (T: +1 801 587 5208; F: +1 801 587 5482; E-mail: Andrew.Anderson@hsc.utah.edu)

© 2016 Orthopaedic Research Society. Published by Wiley Periodicals, Inc.

signs of cam FAI among asymptomatic, healthy hips,^{19,20} which calls into question the ability of radiographic projections and measurements to define anatomical variation specific to this disease. Equally important, assessing the severity of cam FAI using radiographs requires the assumption that a morphologically normal hip is perfectly spherical. Yet, even healthy hips are aspherical.^{21,22} Finally, the projection of complex 3D anatomy to a 2D plane can fail to visualize the magnitude and location of the cam lesion.²³

Correspondence-based computing methods, such as statistical shape modeling (SSM), are powerful tools used to quantify 3D anatomical variation and identify shape differences.^{24–26} Correspondence-based methods are ideal because they do not determine, a-priori, the ideal shape that the structure should conform to. We previously used SSM to demonstrate that cam femora are significantly different in shape compared to controls, and established principal component analysis (PCA) modes that captured the variance in shape.²⁵ In our prior study, a hierarchical splitting strategy was used to automatically place correspondence particles onto the proximal femur. This entropy-based approach to distribute correspondence particles reduces subjectivity as it does not require manual landmark identification or the use of training shapes. From the correspondence model, scalar attributes that accompany shape, such as the thickness of the cortical bone, can be sampled at the same relative anatomic location across a population.

The objective of this study was to use this correspondence-based modeling approach to quantify and compare cortical thickness between cam patients and non-pathologic controls in the location of the cam lesion and throughout the proximal femur. We hypothesized that cam FAI patients would have increased cortical thickness in the region of the cam lesion.

METHODS

Subject Recruitment and Screening

Institutional Review Board (IRB) approval was obtained through the University of Utah (IRBs 11755 and 56086) and Intermountain Healthcare (IRB 1024270). Twenty-eight cam FAI patients (26 males) and 45 control subjects (29 males) of similar age, weight, and body mass index (BMI) were recruited for the study.

Volumetric computed tomography (CT) images of the proximal femur were acquired using a: Siemens SOMATOM 128 Definition CT Scanner (IRB 56086, 20 control subjects, 15 cam patients), GE High Speed CTI Single Slice Helical CT Scanner (IRB 11755, 59 control cadaver femurs), and GE LightSpeed VCT scanner (IRB 1024270, 13 cam patients).²⁵

Patients were diagnosed with cam FAI based on clinical examination and radiographic measurements. Control subjects were selected based on the absence of bony abnormalities. For living control subjects, an anterior–posterior radiograph was read by members of the study team with 5–10 years of medical imaging experience to exclude morphologic abnormalities. For all control femurs, a digitally reconstructed radiograph (DRR) was generated from the CT

images. The alpha angle, which defines the angle between the femoral neck axis and the point at which the femoral head bone deviates laterally from a circle templated onto the radiograph, was measured on the frog-leg lateral DRR. Alpha angles greater than 60° were used to exclude femurs with cam-like morphology.²⁷ A total of 34 out of 79 control femurs were omitted based on these criteria,²⁸ leaving 45 control subjects (15 live subjects and 30 cadaver femurs).

CT datasets were upsampled to axial slice thicknesses of 0.33 mm to improve resolution. Cortical and trabecular bone layers of each proximal femur were semi-automatically segmented and reconstructed from the CT image data using Amira (v5.6, FEI, Hillsboro, OR). Segmentation was completed using the methods of Anderson et al. which previously resulted in less than 10% error for cortical thicknesses greater than 0.7 mm.²⁹ Surfaces were smoothed and decimated in Amira, and then reformatted to visual toolkit (VTK) format.³⁰ Reconstructed surfaces of the two layers were used to determine the thickness of the cortical bone over the surface of the femoral head and proximal shaft using PreView.³¹ Thickness values were calculated using a normal projection from the cortical surface to the trabecular surface and recorded for each node (Fig. 1, top).

Correspondence-Based Shape Modeling

Surfaces representing right femurs were reflected to appear as left femurs and all surfaces were aligned using the iterative closest point algorithm as part of preprocessing.³² ShapeWorks³³ was used to quantify anatomical variation in the shape of the outer cortex, and provided the medium to calculate differences in cortical thickness between groups through modifications to the software framework described below.

ShapeWorks performs analysis on volumetric datasets, and thus requires input of a voxel-based representation of each 3D surface. To accurately represent surfaces using voxels, it is often necessary to reduce voxel size (i.e., increase resolution), which in turn increases the computational size of each volume. To circumvent this issue, a pipeline was developed to accurately generate volume-based representations without the need to reduce the size of each voxel. Here, a spatial partitioning algorithm was used to define a list of candidate surface mesh faces closest to each voxel of a volume. From the list of candidate faces, the nearest triangular face was identified and the physical distance encoded for each voxel of the distance transform (i.e., a volume which includes data of the distance to the nearest surface for each voxel). This technique ensured that the nearest face was chosen using the barycentric distance, which is based on the centers of mass, between each voxel and the surface vertices. The resultant iso-surface (i.e., surface representation generated by connecting the zero-distance voxels) approximated the input surface mesh to an error that did not exceed 0.31 mm using an input voxel size of 0.5 mm.

The primary purpose of this study was to analyze differences in the thickness of the cortex at the proximal femur. To limit placement of correspondence particles to this region, a cutting plane was identified perpendicular to the femoral shaft just proximal to the lesser trochanter for a single template shape. An initial correspondence model, with 512 particles, was used to optimize the transformation of the template plane onto each femur (Fig. 1, middle). Transformed cutting planes were visually verified for

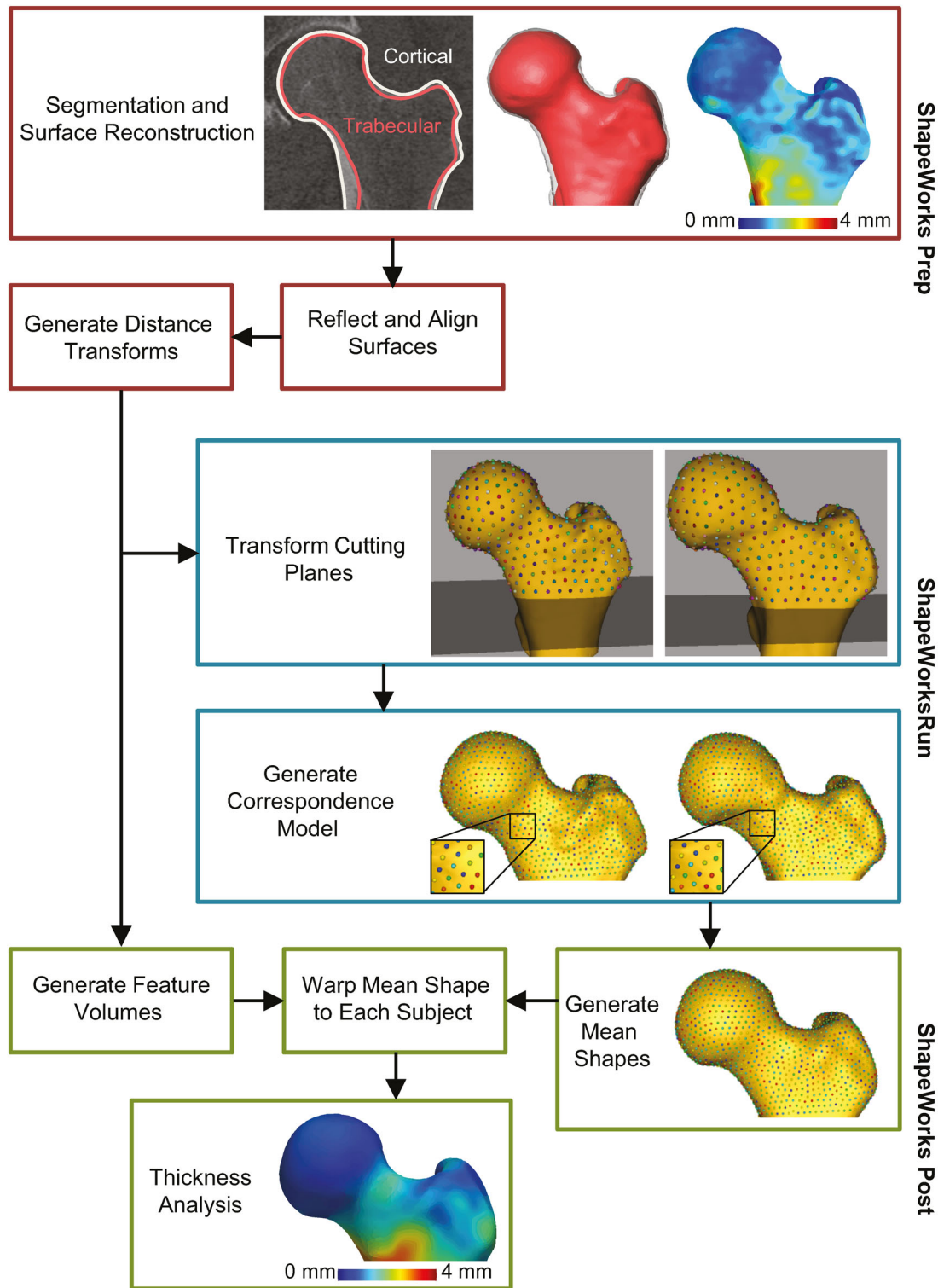


Figure 1. Flowchart for modeling pipeline. Subject specific shapes of the inner and outer boundaries of the cortex were segmented and reconstructed from computed tomography scans; cortical thickness was determined. Surfaces were aligned and rasterized in preparation for analysis. Cutting planes were transformed to each shape and used to limit locations of correspondence points. The correspondence model was generated by placement of particles on each rasterized surface. Mean shapes were calculated from average locations of the correspondence particles. Cortical thickness obtained from each subject was then mapped to the mean shapes of each group using the correspondence model to display variation.

consistency across the population. Correspondence particles ($n = 2,048$) were hierarchically placed above the cutting plane for all shapes using ShapeWorks.^{25,33} The spatial

positions of the particles were optimized based on correspondence across shapes and sampling over each surface (Fig. 1, middle).

The correspondence model and volumetric distance transforms for each subject were used to generate a mean distance transform for the whole population and for each group. The iso-surface generated from this mean distance transform was smoothed and decimated to roughly 50,000 vertices to create the mean surface.^{34,35} Using the correspondence model, the population mean surface was warped to each subject and to the mean shapes of each group using compactly supported radial basis functions,³⁶ which resulted in dense surface meshes for each subject and group that were in correspondence. Using this approach facilitated vertex-to-vertex comparisons, which were necessary to directly compare thickness between shapes.

Volumes of the same dimensions and voxel size as the distance transforms, which represented the 3D femur surface, were generated to include scalar data for each subject, specifically, cortical thickness. This approach could be applied to any feature that accompanies shape. Accordingly, these volumes were referred to as feature volumes. Using the correspondence model, the feature volumes were warped to the mean shapes. Once warped, scalar cortical thickness data for each subject was directly sampled and mapped onto the mean surfaces. From the subject specific cortical thickness data, mean and median values were mapped onto the mean surfaces in Matlab (v7.10, The Mathworks, Inc., Natick, MA). Mean thickness for each group was used in the quantification of group differences, while maximum, median, and mean thicknesses were used for comparison of the subjects within each group. For visualization of cortical thickness variability within groups, thickness at each vertex was sorted to identify the median and 10th, 25th, 75th, and 90th percentile values. These values were mapped onto the surface of the mean cam and control femurs for visualization (Fig. 1, bottom).

The region of the cam lesion was identified to allow for analysis of cortical thickness at the location of surgical resection. The region was identified by first calculating the surface distance between the mean cam and control femur surfaces in PreView.³¹ A region on the femoral head-neck junction, designated by distance greater than 1.5 mm between the mean shapes, was isolated as the region of the cam lesion. A distance of 1.5 mm between shapes isolated a large region of the head-neck junction, while minimizing inclusion of the saddle between the femoral head and the greater trochanter.

Within the region of the cam lesion, the location of maximum thickness was found on both the mean shapes and on each subject specific shape. This location was represented as a vector from the sphere-fit center of the femoral head to the location of maximum thickness and mapped onto each anatomical plane. The best-fit sphere was calculated by first isolating faces of the femoral head based on first principal curvature of the mean cam and control shapes in PostView.³¹ These faces were identified for each subject based on the faces from each respective mean shape. The nodes corresponding to these faces were then fit to a sphere using a linear system of equations in Matlab.

Statistical Analysis

The Shapiro test was used to evaluate normality, and the Wilcoxon rank sum test or Student's *T*-test to evaluate group demographic differences between cam and control subjects in the R statistical software.³⁷ Since there was predominance for male patients, with only two female patients, statistical

analysis was completed to compare not only between cam and control subject populations, but also within control and male populations separately. This resulted in comparisons of cortical bone thickness between female and male control subjects (16 and 29 subjects, respectively) and male cam and control subjects (26 and 29 subjects, respectively).

Principal component analysis (PCA) isolated the modes of variation from the correspondence particle locations. The PCA modes containing significant variation were determined using parallel analysis.³⁸ Within these significant modes, PCA loading values were compared between the two groups using a Student's *T*-test with Finner's adjustment for multiple comparisons.³⁹ Hotelling's T^2 test was utilized to determine whether a significant shape difference existed between the two groups.

The mean correspondence particle locations and thickness values for the mean cam and control femurs were used to generate a linear discrimination between the two shapes in high-dimensional shape space (i.e., high-dimensional vector). Specifically, the 2,048 scalar data points representing cortical thickness at each correspondence particle location were organized into a vector for each subject specific and mean shape. The linear discrimination between the two mean shapes in shape space was then defined as the difference of the two mean shape vectors. Each subject shape was then mapped to this shape space representation by taking the dot product between the subject specific and linear discrimination vectors, which resulted in a single scalar value representation of thickness of each subject shape. This analysis was repeated for the correspondence particle locations to provide a scalar representation of shape. These scalar values were evaluated against shape statistics using Spearman's correlation coefficient.

Maximum, median, and mean cortical thickness values and the angular components of the vector representing the location of maximum thickness were evaluated for normality using the Shapiro-Wilk test and then compared using a Wilcoxon rank sum test or Student's *T*-test with Finner's adjustment for multiple comparisons.

RESULTS

Age and BMI were not normally distributed across the population. Thus, for consistency, all demographics were analyzed using the Wilcoxon rank sum test. The weight of the female controls was significantly less than that of the males ($p = 0.006$); all other metrics between the cam and control populations, male cam and control subgroups, and the female and male control subgroups were not significantly different ($p > 0.05$) (Table 1).

Parallel analysis of the PCA loading values based on the correspondence particle locations on the outer bone cortex identified ten modes of significant variation, which included 85.8% of the total variation within the population, representing 33.5%, 20.4%, 8.3%, 6.4%, 4.7%, 3.9%, 2.6%, 2.4%, 2.1%, and 1.7% of the overall variation, respectively. Three of these modes (PCA modes 1, 5, and 7; Fig. 2) aligned with significant group differences based on analysis of PCA loading values (adj. $p = 0.019$, $p = 0.040$, and $p < 0.001$, respectively). Mode one described general variation in anterior-posterior widths. Modes 5 and 7 represented

Table 1. Demographics for Groups and Subgroups of the Population Represented as Median [Interquartile Range]

	Entire Cohort		Subject Subgroups			
	Controls	Patients	Female Controls	Male Controls	Female Patients*	Male Patients
Subjects, <i>n</i>	45	28	16	29	2	26
Age, years	28 [12]	23 [13]	30 [18]	27 [10]	21, 47	23 [13]
Weight, kg	81.0 [22.0]	81.0 [15.4]	62.8 [22.5]	81.0 [19.0]	68.5, 97.0	81.0 [14.7]
BMI, kg/m ²	24.2 [7.9]	25.0 [3.9]	22.0 [11.3]	25.6 [5.1]	25.9, 32.8	24.8 [4.0]

*Individual values are presented for the female patients due to sample size ($n = 2$).

variations in head–neck offset and femoral head circumference; mode 7 also described variations in the greater trochanter. Modes 2, 3, 4, and 6 represented variations in the curvature of the saddle between the femoral head and greater trochanter, lateral extent of the femoral head and greater trochanter, and shape of the proximal shaft. Hotelling's T^2 test showed the outer cortex of cam and control patient groups to be significantly different in shape ($p < 0.001$).

The scalar mapping of each subject femur onto the linear discrimination of variation in shape space between the cam and control shapes (Fig. 3) showed significant differences between the two groups in terms of both shape (using the three anatomical directions to describe the location of each particle) and thickness (using the scalar thickness value at each particle) ($p < 0.001$ for both). Mode one from PCA was strongly correlated to the shape mapping ($r = 0.94$, adj. $p < 0.001$); all other modes had no more than a weak correlation and were not significant after correction for multiple comparisons ($r < 0.15$, adj. $p > 0.684$). The thickness mapping values were weakly correlated with PCA modes 1, 2, 3, 6, 7, and 8, but were not significant after correction for multiple comparisons ($r < 0.29$; adj. $p > 0.118$ for all). The shape and thickness mappings were also weakly correlated ($r = 0.37$, $p = 0.001$).

Thickness data were not normally distributed. Thus, a Wilcoxon rank sum test was used for comparison of subject thickness metrics. Cam patients had increased cortical thickness compared to control subjects in terms of maximum, median, and mean thickness values within the region of the cam lesion, as identified by shape differences (Fig. 4, top right), and median thickness values over the proximal femur,

whether gender effects were considered or not (Table 2). No difference in cortical thickness was evident between male and female control subjects.

When comparing thickness between mean shapes (one-to-one comparison, no p -values), qualitative inspection revealed increased cortical thickness in patients with cam FAI for the region of the cam lesion. The region of the cam lesion was also thicker on average than the entire proximal femur. Overall, the mean proximal cam femur was thicker than the mean control femur (Table 3). The maximum thickness of the cam lesion was greater for cam patients than controls (2.47 vs. 1.71 mm). The maximum difference in thickness between the two mean shapes was within the region of the cam lesion and 1.35 mm in magnitude (Fig. 4, bottom right). The mean cam shape had greater cortical thickness throughout the entire cam lesion.

The mean female control and male cam femurs were also thicker than the mean male control femur (Table 3). Among the mean male shapes, the maximum thickness within the region of the cam lesion was 2.53 and 1.65 mm for the cam and control subjects, respectively. The male cam shape had greater thickness throughout the entire region with a maximum difference in thickness of 1.47 mm. Among the controls, the maximum thickness for the female controls was greater than that of the male controls (1.91 vs. 1.65 mm, respectively). The female control shape was maximally 0.48 mm thicker and 0.19 mm thinner than the male control shape within the region identified as the cam lesion.

Median regional thickness, evaluated within the region of the cam lesion, for each subject was moder-

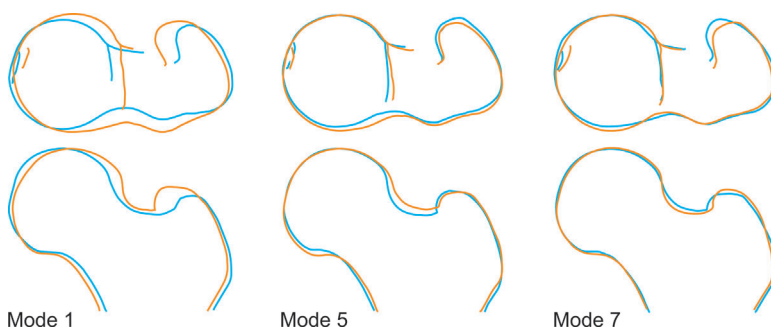


Figure 2. Contours representing the 2D projection of femur surfaces in the axial and coronal planes represent variation of plus (blue) and minus (orange) two standard deviations of each PCA mode that corresponded to a significant difference between the cam and control shapes. Modes represent variation in the curvature of the femoral head–neck junction and greater trochanter.

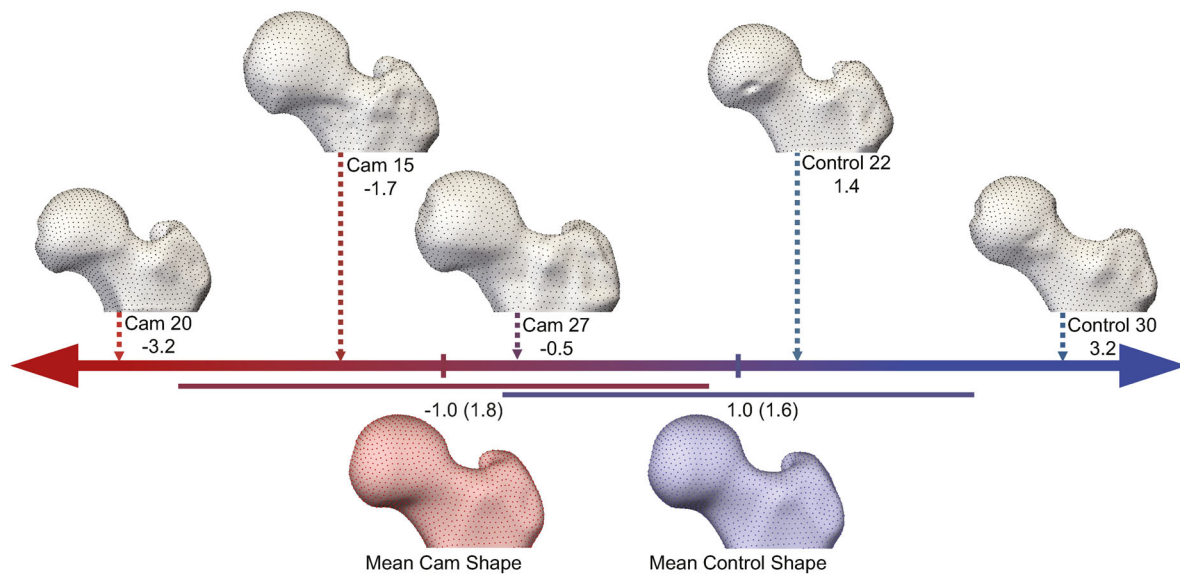


Figure 3. The correspondence model was used to determine a linear discrimination of the variation between the mean cam and mean control shapes in shape space (bottom row) which was normalized from -1 to $+1$. Standard deviations for each are shown in parentheses and mapped above the mean shapes. Each subject shape was then mapped to this linear representation of shape variabilities. Five subject specific shapes from three cam patients and two controls are shown with their mapping value at the appropriate location.

ately correlated with the thickness mapping ($r = 0.66$, $p < 0.001$). When comparing the PCA loading values for each significant mode of variation to the median thickness within the region of the cam lesion, a weak correlation with PCA mode 6 was identified ($r = 0.38$, adj. $p = 0.015$). No other correlations between thickness and shape statistics were found to be significant.

Median and percentile thickness values mapped onto the mean cam and control femurs showed a large region of variable thickness for the cam femur with minimal increase in thickness for the lower percentiles and clear increases in thickness for the higher percentiles (Fig. 5).

The vector between the femoral head center and the location of maximum thickness was directed more anterior and less inferior in patients compared to controls (median [interquartile range]; $46 [24]^\circ$ vs. $30 [19]^\circ$ anterior of lateral and $10 [25]^\circ$ vs. $21 [26]^\circ$ inferior of anterior; adj. $p = 0.016, 0.039$, respectively; Fig. 6). The coronal components of this vector were not significantly different between the two groups ($9 [29]^\circ$ vs. $11 [19]^\circ$ inferior of lateral; adj. $p = 0.635$). When comparing the subgroups, similar results were seen for the male cam and control groups in the axial plane, with components of $46 (22)^\circ$ versus $30 (21)^\circ$ anterior of lateral (adj. $p = 0.009$). The location of maximum cortical thickness was less inferior in the sagittal plane ($17 [26]^\circ$ vs. $28 [17]^\circ$, adj. $p = 0.044$) in males than females in the control group. The vectors to maximum thickness for the mean cam and control shapes differed by 11° in the axial, 6° in the sagittal, and 0° in the coronal plane between the two groups, which agreed well with the differences identified based on the vectors identified on subject specific shapes.

DISCUSSION

Correspondence-based shape modeling was used to identify the region of the cam lesion based on shape variation between cam and control subjects. Cortical bone thickness in this region of the femur, as well as over the proximal surface, was significantly greater in patients with cam FAI than control subjects. The location of maximal cortical thickness was variable, but was more anterior and less inferior in patients. Cortical thickness magnitude was not significantly different between male and female control populations, but the location was less inferior in males. Similar to the population of cam and control subjects, the male cam and control groups showed significant differences in both maximum thickness and location of maximum cortical thickness in the axial plane.

The increase in thickness of cortical bone in the region of the cam lesion could be the result of hypertrophy due to a biological response to the repetitive impingement associated with deep flexion, internal rotation, and adduction.^{3,14} This concept agrees with a previous study, which identified increased bone density of the subchondral bone in patients with cam FAI.⁴⁰ To understand the biomechanical and biological effect of impingement, additional focus should be placed on cortical bone thickness in the corresponding region of the acetabulum, as increased bone density has been identified in this region and hypothesized to be a factor in osteoarthritis development.⁴¹ Interestingly, we found that thickness of the entire proximal femur was greater in cam FAI patients. This could indicate generalized bone hypertrophy, possibly due to an adaptation of the entire femur due to altered loading at the primary impingement site.

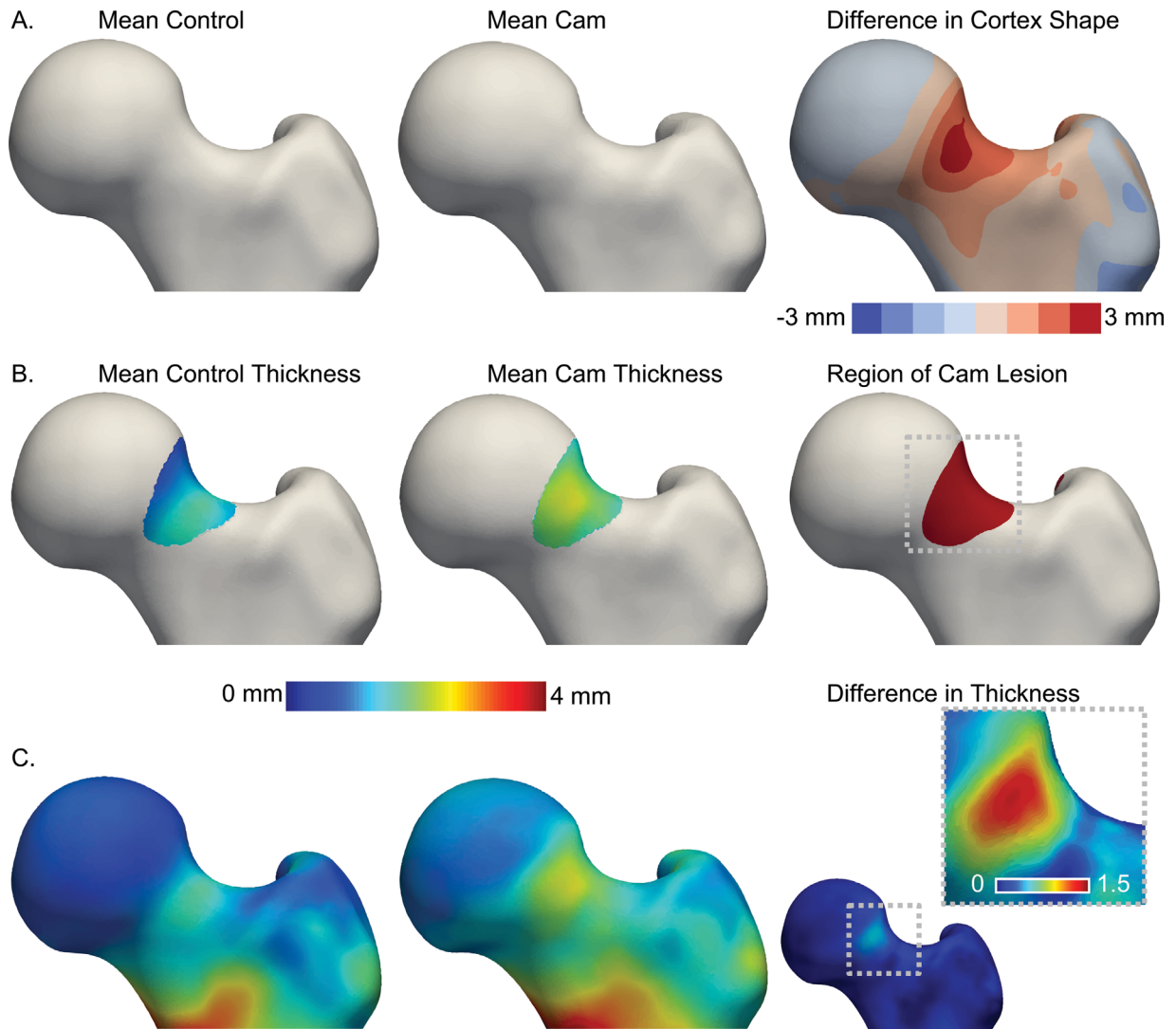


Figure 4. Anterior view of fringe plots showing differences in anatomy and mean cortical thickness for cam and control groups. (A) Mean shapes for the control (left) and cam (middle) groups shown with the shape difference mapped onto the mean control femur (right). (B) The region of the head-neck junction with greater than 1.5mm of difference in the anatomy of the outer cortex was identified as the region of the cam lesion (right); thickness was evaluated for this region on the mean control (left) and cam (middle) shapes. (C) Mean cortical thickness of the control (left) and cam (middle) groups with the difference in mean thickness between groups (right). The greatest difference in thickness corresponded with the region of the cam lesion (right, inset). Note: The fringe plot in the inset has been re-scaled.

Results demonstrating the variability in thickness over the population could indicate that the proximal femur is stronger in cam FAI patients, due to increased cortical thickness. Specifically, for percentiles greater than the median, there was a clear increase in cortical thickness on the femoral neck near the region of the cam lesion and on the proximal medial femoral shaft. These increases in cortical thickness were much more obvious in the cam group than the control group. A small region of increased thickness could be seen on the mean control femur, although it was positioned more distally on the femoral neck than on the cam femur. This increase indicates some natural variability in cortical thickness over the femoral neck, even in the asymptomatic population. It will be important to confirm that cam femurs have increased strength due to elevated cortical

thickness, as these mechanical data could help to refine guidelines pertaining to the optimal resection depth.

The general shape variations between cam FAI and control femurs agree with our prior research identifying shape variations at the head-neck junction and greater trochanter.²⁵ However, the content of each specific PCA mode varied. This difference in PCA modes is likely due to differences in alignment and cropping. Since the cutting planes were transformed onto each femur based on an initial optimized correspondence model, the plane location would have reduced the variability in vertical distance to the greater trochanter and any angular variations of the shaft. These variabilities may be important when evaluating shape variation of the proximal femur, but are likely not necessary in the evaluation of cortical

Table 2. Median and Interquartile Range (IQR) of Subject Specific Maximum, Median, and Mean Regional and Median Proximal Femur Thickness for All Groups and Subgroups

Entire Cohort			Subject Subgroups	
	Median [IQR]	adj. <i>p</i>	Median [IQR]	adj. <i>p</i>
Maximum regional thickness, mm				
Controls	2.30 [1.13]		Male controls	2.62 [1.20]
			Female controls	2.24 [0.59]
			Male patients	3.47 [2.50]
Patients	3.47 [2.23]	<0.001	Female patients	2.88, 4.13
Mean regional thickness, mm				
Controls	1.18 [0.31]		Male controls	1.17 [0.29]
			Female controls	1.21 [0.38]
			Male patients	1.71 [0.79]
Patients	1.71 [0.81]	<0.001	Female patients	1.15, 1.92
Median regional thickness, mm				
Controls	1.13 [0.22]		Male controls	1.10 [0.19]
			Female controls	1.13 [0.34]
			Male patients	1.47 [0.72]
Patients	1.47 [0.64]	<0.001	Female patients	0.86, 1.63
Median proximal femur thickness, mm				
Controls	0.97 [0.22]		Male controls	0.94 [0.22]
			Female controls	0.99 [0.17]
			Male patients	1.25 [0.29]
Patients	1.28 [0.30]	<0.001	Female patients	1.77, 1.28

IQR indicates variation within each group. Regional thickness was evaluated within the region of the cam lesion. *p*-values shown are relative to control and male control groups for the entire cohort and subject subgroups, respectively. *No statistical comparisons were made with the female patient group due to sample size ($n = 2$).

thickness, especially for the region of the cam lesion. Further, reduced variability within the region of analysis may have helped to elucidate more subtle differences in this area.

For this study, we evaluated the cam lesion in the context of the entire proximal femur; this was done for several reasons. First and foremost, in addition to testing the hypothesis that cortical bone was thicker in the region of the cam lesion, we sought to determine if the entire proximal femur had increased cortical thickness. If we had isolated the analysis only to the region of the cam lesion, we would not have had the

ability to evaluate differences over the proximal femur. Second, the region of the cam lesion represents only a small region of the femoral head and head-neck region, which is not normal anatomy. Without reference to nearby anatomy, it would be difficult to justify how any specific lesion or part of a lesion would relate to another lesion. The goal of this work was to evaluate the cam lesion and cortical thickness by virtue of their deviation from normal anatomy. Manually defining the lesions a-priori would not enable this objective quantification. In terms of technical issues, although our method to optimize the placement of

Table 3. Median and Interquartile Range (IQR) of Regional and Overall Thickness for Mean Shapes for All Groups and Subgroups

Entire Cohort	Median [IQR]	Subject Subgroups	Median [IQR]
Mean shape regional thickness, mm			
Controls	1.26 [0.48]	Male controls	1.23 [0.44]
		Female controls	1.28 [0.57]
Patients	1.91 [0.41]	Male patients	1.92 [0.44]
		Female patients	1.69 [0.95]
Mean shape overall thickness, mm			
Controls	1.02 [0.49]	Male controls	1.01 [0.49]
		Female controls	1.04 [0.49]
Patients	1.33 [0.52]	Male patients	1.32 [0.52]
		Female patients	1.52 [0.78]

IQR indicates the variation in mean thickness for each mean shape. Regional thickness was evaluated within the region of the cam lesion. *p*-values shown are relative to control and male control groups for the entire cohort and subject subgroups, respectively.

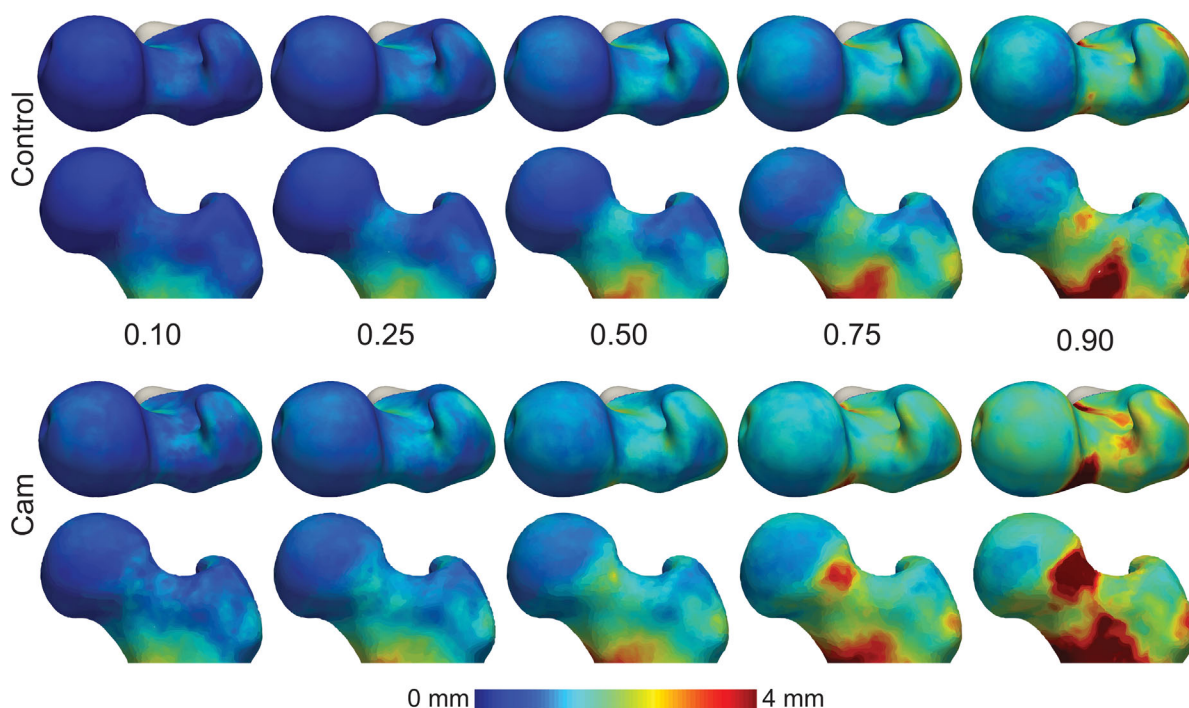


Figure 5. Percentile thickness representing the 10th, 25th, 50th, 75th, and 90th percentile of thickness for each of the vertices on the mean control (top) and cam (bottom) femur (median thickness is the 50th percentile). Increased cortical thickness was evident overall and in the region of the cam lesion on the mean cam femur.

correspondence particles is automatic, it does require unique anatomical features to ensure that correspondence particles are positioned across samples in the same relative anatomic position. Thus, it would be difficult to estimate correspondences on these isolated patches without the benefit of reference to nearby anatomy.

Each PCA mode is an objective measure that considers the entire shape space; it does not directly measure any single aspect of the anatomy that is

clinically relevant, such as the shape of the head–neck junction. Since PCA was performed based on the entire proximal femur, it is important to note that each PCA mode described some aspect of shape variation of the proximal femur, but none were specific to the region of the cam lesion. Accordingly, it should not be surprising that PCA loading values were not strongly correlated with regional thickness metrics or the mapping of thickness between the mean cam and control shapes. While a strong correlation between thickness and a specific mode of variation would have identified shape variations, which could be used to identify increased cortical thickness clinically, a lack of correlation does not signify that shape and thickness are not related; cortical thickness in the region of the cam lesion was clearly increased in cam patients compared to controls.

Previous studies have identified gender differences in the presentation of FAI including variations in radiographic measurements and intraoperative pathology,⁴² which motivate analysis of cortical thickness specific to gender. The cam group only included two female subjects, and thus, statistically meaningful comparisons could not be made directly for female cam shapes. Our recruitment of control subjects was also imbalanced to include more males than females, with only 16 females compared to 29 males, since cam FAI is predominantly seen in males.⁴² It is possible that with a larger number of female control subjects and better sampling of the population, differences in cortical thickness due to gender would be more evident. However, based on the data available, the gender differences in cortical thickness are of smaller magnitude

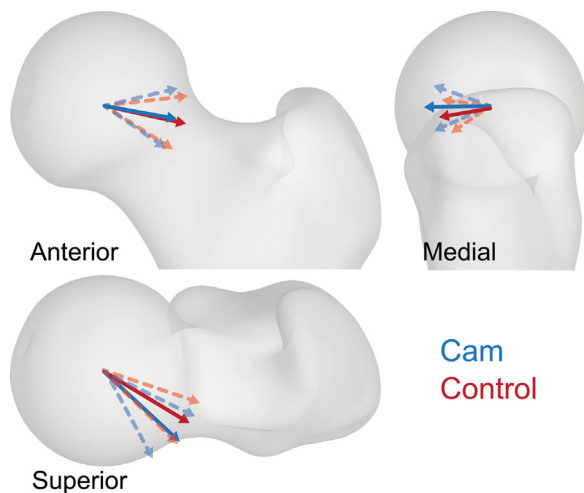


Figure 6. Vectorial representation of the location of maximum cortical bone thickness plotted relative to the mean shape of the control group. Solid vectors represent mean location for the cam (blue) and control (red) groups. Dashed vectors represent one standard deviation of angular variation in each view.

than differences between the cam and control group. Thus, similar increases in cortical thickness could be expected in females with cam-type FAI.

The location of maximum thickness within the region of the cam lesion was variable across the populations. Most of the variation between groups could be captured in the axial plane with the location of maximum cortical thickness more anterior and less lateral in patients with cam FAI. A more anterior location of maximum cortical thickness could indicate bone hypertrophy caused by repetitive abutment during hip flexion and internal rotation.⁴ Within the cam group the variation in each anatomic plane was high. This variability signifies the difficulty in generalizing the cam lesion across patients with cam FAI and justifies subject specific surgical planning.

Improved accuracy in the generation of volumetric distance transforms from surface data facilitates future biological and biomechanical studies where surface meshes are commonly used. The inclusion of reflection and alignment tools herein provided efficient and automated preprocessing to reduce manual time requirements in generation of the correspondence model. The automatic transformation of cutting planes could be extended to analysis of larger populations where a particular anatomical location is of primary interest. Advancements in warping techniques, which incorporate the correspondence model and original distance transforms, allow for direct vertex-to-vertex comparisons between both subject and mean shapes. Additionally, the incorporation of scalar attributes in shape analysis could be adapted to other applications. For this study, a scalar value was used to represent cortical bone thickness, but future studies could use this technique to evaluate other attributes that accompany shape, such as bone densities from CT data or stresses from finite element analysis.

While we did not find strong correlative relationships between shape and cortical bone thickness, it is clinically important to understand that cortical bone thickness is increased proximally and in the region of the cam lesion for patients with cam FAI. Previous studies evaluating resection depth have not taken into account possible variations in cortical thickness for patients with cam FAI.^{11–13} Additional research is required to establish parameters of the resection to prevent both under-resection and iatrogenic femoral neck fractures that are specific to the anatomical characteristics in patients with cam FAI.¹⁰

AUTHORS' CONTRIBUTIONS

PRA processed data, conducted the study, and drafted the manuscript. SE and PA implemented the software to complete the study and reviewed the results for accuracy. MH collected and processed the original data and interpreted study results. RW, JW, and CP contributed to the design of the study, assisted with clinical interpretation, and reviewed the results for accuracy. AA designed the study, supervised the study, reviewed the results for accuracy, and assisted

with clinical interpretation. All authors provided revisions and final approval of the manuscript.

ACKNOWLEDGMENTS

The research content herein is solely the responsibility of the authors and does not necessarily represent the official views of the National Institutes of Health. The authors also acknowledge Trevor Hafer and Tyler Skinner.

REFERENCES

- Murphy LB, Helmick CG, Schwartz TA, et al. 2010. One in four people may develop symptomatic hip osteoarthritis in his or her lifetime. *Osteoarthritis Cartilage* 18:1372–1379.
- Beck M, Kalhor M, Leunig M, et al. 2005. Hip morphology influences the pattern of damage to the acetabular cartilage femoroacetabular impingement as a cause of early osteoarthritis of the hip. *J Bone Joint Surg Br* 87:1012–1018.
- Ganz R, Leunig M, Leunig-Ganz K, et al. 2008. The etiology of osteoarthritis of the hip. *Clin Orthop Relat Res* 466:264–272.
- Ganz R, Parvizi J, Beck M, et al. 2003. Femoroacetabular impingement: a cause for osteoarthritis of the hip. *Clin Orthop Relat Res* 417:112–120.
- Wagner S, Hofstetter W, Chiquet M, et al. 2003. Early osteoarthritic changes of human femoral head cartilage subsequent to femoro-acetabular impingement. *Osteoarthritis Cartilage* 11:508–518.
- Kapron AL, Anderson AE, Peters CL, et al. 2012. Hip internal rotation is correlated to radiographic findings of cam femoroacetabular impingement in collegiate football players. *Arthroscopy* 28:1661–1670.
- Kapron AL, Aoki SK, Peters CL, et al. 2014. Subject-specific patterns of femur-labrum contact are complex and vary in asymptomatic hips and hips with femoroacetabular impingement. *Clin Orthop Relat Res* 472:3912–3922.
- Kapron AL, Aoki SK, Peters CL, et al. 2015. In-vivo hip arthrokinematics during supine clinical exams: application to the study of femoroacetabular impingement. *J Biomech* 48:2879–2886.
- Philippon MJ, Schenker ML, Briggs KK, et al. 2007. Revision hip arthroscopy. *Am J Sports Med* 35:1918–1921.
- Ayeni OR, Bedi A, Lorich DG, et al. 2011. Femoral neck fracture after arthroscopic management of femoroacetabular impingement: a case report. *J Bone Joint Surg Am* 93:e47.
- Mardones RM, Gonzalez C, Chen Q, et al. 2005. Surgical treatment of femoroacetabular impingement: evaluation of the effect of the size of the resection. *J Bone Joint Surg Am* 87:273–279.
- Rothenfluh E, Zingg P, Dora C, et al. 2012. Influence of resection geometry on fracture risk in the treatment of femoroacetabular impingement: a finite element study. *Am J Sports Med* 40:2002–2008.
- Wijdicks CA, Ballin BC, Jansson KS, et al. 2013. Cam lesion femoral osteoplasty: in vitro biomechanical evaluation of iatrogenic femoral cortical notching and risk of neck fracture. *Arthroscopy* 29:1608–1614.
- Robling AG, Castillo AB, Turner CH. 2006. Biomechanical and molecular regulation of bone remodeling. *Annu Rev Biomed Eng* 8:455–498.
- Holzer G, von Skrbensky G, Holzer LA, et al. 2009. Hip fractures and the contribution of cortical versus trabecular bone to femoral neck strength. *J Bone Miner Res* 24:468–474.
- Ito K, Minka-II M-A, Leunig M, et al. 2001. Femoroacetabular impingement and the cam-effect a MRI-based quantitative anatomical study of the femoral head-neck offset. *J Bone Joint Surg Br* 83:171–176.

17. Sutter R, Zanetti M, Pfirrmann CW. 2012. New developments in hip imaging. *Radiology* 264:651–667.
18. Tannast M, Siebenrock KA, Anderson SE. 2007. Femoroacetabular impingement: radiographic diagnosis—what the radiologist should know. *Am J Roentgenol* 188:1540–1552.
19. Hack K, Di Primio G, Rakhra K, et al. 2010. Prevalence of cam-type femoroacetabular impingement morphology in asymptomatic volunteers. *J Bone Joint Surg Am* 92:2436–2444.
20. Kapron AL, Anderson AE, Aoki SK, et al. 2011. Radiographic prevalence of femoroacetabular impingement in collegiate football players: aAOS exhibit selection. *J Bone Joint Surg Am* 93:e111.
21. Anderson AE, Ellis BJ, Maas SA, et al. 2010. Effects of idealized joint geometry on finite element predictions of cartilage contact stresses in the hip. *J Biomech* 43:1351–1357.
22. Menschik F. 1997. The hip joint as a conchoid shape. *J Biomech* 30:971–973.
23. Meyer DC, Beck M, Ellis T, et al. 2006. Comparison of six radiographic projections to assess femoral head/neck asphericity. *Clin Orthop Relat Res* 445:181–185.
24. Dudda M, Albers C, Mamisch TC, et al. 2009. Do normal radiographs exclude asphericity of the femoral head-neck junction? *Clin Orthop Relat Res* 467:651–659.
25. Harris MD, Datar M, Whitaker RT, et al. 2013. Statistical shape modeling of cam femoroacetabular impingement. *J Orthop Res* 31:1620–1626.
26. Harris MD, Kapron AL, Peters CL, et al. 2014. Correlations between the alpha angle and femoral head asphericity: implications and recommendations for the diagnosis of cam femoroacetabular impingement. *Eur J Radiol* 83:788–796.
27. Clohisy JC, Nunley RM, Otto RJ, et al. 2007. The frog-leg lateral radiograph accurately visualized hip cam impingement abnormalities. *Clin Orthop Relat Res* 462:115–121.
28. Sutter R, Dietrich TJ, Zingg PO, et al. 2012. How useful is the alpha angle for discriminating between symptomatic patients with cam-type femoroacetabular impingement and asymptomatic volunteers? *Radiology* 264:514–521.
29. Anderson AE, Peters CL, Tuttle BD, et al. 2005. Subject-specific finite element model of the pelvis: development, validation and sensitivity studies. *J Biomech Eng* 127:364–373.
30. Schroeder W, Martin K, Lorensen B, editors. 2006. *The visualization toolkit*, 4th ed. Clifford Park, NY, USA: Kitware.
31. Maas SA, Ellis BJ, Ateshian GA, et al. 2012. FEBio: finite elements for biomechanics. *J Biomech Eng* 134:011005.
32. Besl PJ, McKay HD. 1992. A method for registration of 3-D shapes. *IEEE Trans Pattern Anal Mach Intell* 14:239–256.
33. Cates J, Fletcher PT, Styner M, et al. 2007. Shape modeling and analysis with entropy-based particle systems. *Inf Process Med Imaging* 20:333–345.
34. Sorkine O, Cohen-Or D, Lipman Y, et al. 2004. Laplacian surface editing. *Proceedings of the 2004 Eurographics/ACM SIGGRAPH symposium on geometry processing*. Nice, France: ACM. p 175–184.
35. Valette S, Chassery JM, Prost R. 2008. Generic remeshing of 3D triangular meshes with metric-dependent discrete Voronoi diagrams. *IEEE Trans Vis Comput Graph* 14:369–381.
36. Zhu S-X. 2012. *Compactly supported radial basis functions: how and why?* Technical report. Oxford, England: The Mathematical Institute, University of Oxford.
37. RCoreTeam. 2014. *R: a language and environment for statistical computing*. Vienna, Austria: R Foundation for Statistical Computing.
38. Horn JL. A rationale and test for the number of factors in factor analysis. *Psychometrika* 30:179–185.
39. Finner H. 1993. On a monotonicity problem in step-down multiple test procedures. *J Am Statist Assoc* 88:920–923.
40. Speirs AD, Beaulé PE, Rakhra KS, et al. 2013. Bone density is higher in cam-type femoroacetabular impingement deformities compared to normal subchondral bone. *Osteoarthritis Cartilage* 21:1068–1073.
41. Speirs A, Beaulé P, Rakhra K, et al. 2013. Increased acetabular subchondral bone density is associated with cam-type femoroacetabular impingement. *Osteoarthritis Cartilage* 21:551–558.
42. Nepple JJ, Riggs CN, Ross JR, et al. 2014. Clinical presentation and disease characteristics of femoroacetabular impingement are sex-dependent. *J Bone Joint Surg Am* 96:1683–1689.